AIAA 82-4115

Scale Effects on Cavitating Flows Due to Surface Roughness and Laminar Separation

Michael L. Billet,* J. William Holl,† and Blaine R. Parkin†
The Pennsylvania State University, State College, Pa.

Roughness and viscous scale effects are an important consideration when using model data to predict limited cavitation on a prototype, since in many cases the limited cavitation number of a model is different from that of the prototype. In this paper it is shown that fixed patch cavitation, which is observed on axisymmetric headforms and sheet cavitation observed on hydrofoils, may be controlled by surface roughness. An analysis predicts the same general characteristics as that shown by the experimental data; namely, the cavitation number increases with Reynolds number *Re* for a given size and increases with decreasing size for a given value of *Re*. The results of a theoretical analysis of bubble-ring cavitation on a hemispherical nose are also presented. The analysis, which indicates that both Reynolds number and Weber number are important scaling parameters, is employed in an attempt to correlate extensive experimental data.

Introduction

INSPECTION of several sets of data for limited surface cavitation on hydrofoils and headforms has indicated a common characteristic; namely, the desinent cavitation number σ_d increases with Reynolds number for constant body size and increases with decreasing size for constant Reynolds number. Scale effects of this type may be due to isolated surface roughness, as shown by an analysis in this paper. In addition, the results of an analysis of bubble-ring cavitation caused by laminar separation on a hemispherical nose suggests that the observed scale effects may be due to the influence of both Reynolds number and Weber number.

Let us, first of all, present the essential features of scale effects due to an isolated surface roughness. This will subsequently be applied to hydrofoil and headform data. A summary of the analysis of bubble-ring cavitation and its application to headform data will follow the presentation of the roughness effects analysis.

As indicated by Holl,[1] the limited cavitation number (or desinent cavitation number) for a body with roughness σ_{tr} is given by the superposition equation

$$\sigma_{tr} = -\bar{C}_p + [1-\bar{C}_p]\sigma_{tfp} \tag{1}$$

where $\bar{C}_p$ is the mean pressure coefficient at the location of the roughness on the "smooth" body and σ_{tfp} is the limited cavitation number of the roughness as determined from flat plate data. Equation (1) assumes that cavitation occurs when the minimum pressure $P_{\min-r}$ equals vapor pressure P_v. Arndt et al.[2] have revised this equation to include possible bubble dynamic effects. The revised equation is

$$\sigma_{tr} = -\bar{C}_p - \Omega + [1-\bar{C}_p]\sigma_{tfp} \tag{2}$$

The function Ω accounts for possible bubble dynamic effects and is defined as

$$\Omega = \frac{P_v - P_{\min-r}}{\frac{1}{2}\rho U_\infty^2} \tag{3}$$

where $P_{\min-r}$ is the minimum pressure produced by the roughness and P_v is the vapor pressure.

We will assume that the cavitation is controlled by an isolated surface roughness of height h in a boundary layer of thickness δ. It has been shown[2] that for such irregularities, the cavitation number is approximated by an equation of the form

$$\sigma_{tfp} = C_1 (h/\delta)^a (U\delta/\nu)^b \tag{4}$$

where U, the velocity at the edge of the boundary layer, is given by

$$\frac{U}{U_\infty} = \sqrt{1-\bar{C}_p} \tag{5}$$

The empirical constants a, b, and C_1 depend upon the shape of the roughness.

The boundary-layer thickness δ is approximated by an equation of the form

$$\delta/X = C_2 (U_\infty X/\nu)^{-(1/m)} \tag{6}$$

where X is the streamwise distance from the stagnation point.

Employing Eqs. (5) and (6) in Eq. (4), one finds

$$\sigma_{tfp} = \frac{C_1}{C_2^{(a-b)}} \left(\frac{h}{L}\right)^a \frac{(U_\infty L/\nu)^{[(a-b/m)+b]}}{(X/L)^{(m-1/m)(a-b)}} (1-\bar{C}_p)^{b/2} \tag{7}$$

where L is a characteristic body length, such as chord, diameter, etc. Assuming that the roughness occurs at the same relative point, i.e., X/L is a constant, one finds that Eq. (7) will reduce to a relation of the form

$$\sigma_{tfp} = C_3 (h/L)^a (U_\infty L/\nu)^{C_4} \tag{8}$$

where C_3, C_4, and a are positive constants. Using Eq. (8) in Eq. (2), one obtains the result

$$\sigma_{tr} = -\bar{C}_p - \Omega + C_5 (h/L)^a (U_\infty L/\nu)^{C_4} \tag{9}$$

Thus, if h is a constant, then σ_{tr} increases with Reynolds number for constant L and increases with a decrease in L for constant Reynolds number. In the next section, it will be indicated that several sets of scaling data for both hydrofoils and headforms, display this trend and Eq. (9) will be used to analyze some of these data.

Received Jan. 26, 1981; revision received Aug. 11, 1981. This paper is declared a work of the U. S. Government and therefore is in the public domain.

*Research Associate, Applied Research Laboratory. Member AIAA.

†Professor of Aerospace Engineering, Applied Research Laboratory. Associate Fellow AIAA.

Cavitation Data

In the literature there are many examples of limited cavitation data that show a common characteristic; namely, the cavitation number increases with Reynolds number *Re* for constant size and increases with decreasing size for a fixed value of *Re*. These data, from Refs. 3-6, are from tests on both hydrofoils and headforms and are listed in Table 1.

Although all of the cases listed in Table 1 show the aforementioned common characteristic, the physical appearance of the cavitation has not been documented in all cases. Sheet cavitation was observed on the leading edge of the NACA 0015 hydrofoil and was characterized by small, fixed patches with triangular leading edges distributed across the span. This characteristic suggests possible roughness effects. According to Arakeri and Acosta,[7] the critical Reynolds number for the hemispherical nose is 5×10^6, which corresponds to a velocity of 22.8 ms on a 203.2-mm-diam nose at 24°C. Thus, almost the entire range of flow states indicated in Table 1 for this nose is influenced by laminar separation. However, as indicated by Parkin and Holl,[3] the 101.6- and 203.2-mm-diam hemispheres were characterized by small, fixed patches of cavitation which, as in the case of the NACA 0015 hydrofoil, suggests possible surface roughness effects. Also, since the physical appearance of the cavitation on the 101.6 and 203.2 mm noses was similar to that observed for the NACA 0015 hydrofoil rather than that of band or bubble-ring cavitation which occur in laminar separation bubbles,[8] one suspects that the actual critical Reynolds number for these experiments is somewhat less than 5×10^6.

The NACA 0015 hydrofoil data and 101.6 and 203.2 mm hemispherical nose data will be analyzed in the following section using an analysis based on cavitation produced by an isolated roughness. At lower Reynolds numbers, bubble-ring cavitation was observed on the hemispherical nose suggesting laminar separation effects. These will be examined in a subsequent section.

Scale Effect Due to Roughness

Limited cavitation occurs near the leading edge of the NACA 0015 hydrofoil. In this region, the boundary layer is very thin so that surface roughness could be of major importance. The result of the analysis on roughness effects given by Eq. (9) can be utilized to predict the trends observed for limited cavitation on the NACA 0015 hydrofoil.

Table 1 Sources of cavitation data

Body	Size range	*Re* range	Reference
Hemispherical nose	6.3-203.2 mm diam	1×10^5 to 6.5×10^6 (*Re* based on diameter)	3
1.5 caliber ogive	12.7-101.6 mm diam	2.3×10^5 to 3.5×10^6 (*Re* based on diameter)	3
0.5 caliber hydrofoil	50.8-127.0 mm chord	4×10^5 to 3.5×10^6 (*Re* based on chord)	4
Joukowski hydrofoil	50.8-203.2 mm chord	5×10^5 to 6.5×10^6 (*Re* based on chord)	5
NACA 0015 hydrofoil	38.1-304.8 mm chord	4×10^5 to 6×10^6 (*Re* based on chord)	6
Symmetrical Joukowski hydrofoil	38.1-304.8 mm chord	3.5×10^5 to 6×10^6 (*Re* based on chord)	6
Cambered hydrofoil with quasi-elliptical planform (NACA 0010)	38.1-304.8 mm chord	4×10^5 to 5×10^6 (*Re* based on chord)	6

In this analysis, the characteristic body length would be the hydrofoil chord and the $\bar{C}_p$ would be $\bar{C}_{p_{\min}}$ since the pressure minimum would be near the leading edge. A value of $-\bar{C}_{p_{\min}}=1.4$ at $X/C=0.10$ was calculated for these hydrofoils.

The hydrofoils were machined so that the cutter ran parallel to the leading edge of the hydrofoil. Thus, let us assume that the roughness would be an isolated two-dimensional triangle. This assumption is based on the observation of attached patch or spot cavitation for limited cavitation on the hydrofoils. From Ref. 2, the empirical constants for the triangular roughness are $C_1=0.152$, $a=0.361$, and $b=0.196$. The boundary layer is assumed to be turbulent so that $m=5$, and it is assumed that $C_2=0.38/2$ to account for an initial laminar boundary layer. The maximum height (h) of the roughness is estimated to be 2.54×10^{-3} mm.

Employing these data in Eqs. (7) and (2) and adjusting Ω so that σ_{i_r} agrees with the experimental data at a chord length of 152.4 mm and Reynolds number of 1.5×10^6, one finds that

$$\sigma_{i_r}=1.4-0.445+0.706(h/C)^{0.361}(U_\infty C/\nu)^{0.229} \tag{10}$$

The results of this calculation are shown by the dashed lines in Fig. 1. It is seen that the Reynolds number effect is larger than predicted by Eq. (10). A reasonably good empirical fit to these data is given by

$$\sigma_{i_r}=1.4-0.92+0.1(h/C)^{0.15}(U_\infty C/\nu)^{0.27} \tag{11}$$

which is shown by the solid lines in Fig. 1. In terms of the exponents in these two power-law equations, the empirical fit has a slightly greater dependence on Reynolds number but less than half the dependence on the roughness height compared to Eq. (10).

The characteristic body length would be the diameter for correlating the 101.6 and 203.2 mm hemispherical nose data. The value of $C_{p_{\min}}$ is -0.74. Thus, Eq. (11) was used in the form

$$\sigma_{i_r}=0.74-\Omega+A(h/D)^{0.15}(U_\infty D/\delta)^{0.27} \tag{12}$$

The constants Ω, A were obtained by using experimental data and were found to be $\Omega=0.39$ and $A=0.031$. Again, the roughness height was assumed to be $h=2.54\times10^{-3}$ mm. This correlation, shown by the solid lines, compares very favorably with the experimental data in Fig. 2.

The trends obtained by using a roughness scale effect correlation for attached-spot-type cavitation do parallel the experimental data. The fact that both the hydrofoils and hemispherical noses have the same Reynolds number and relative roughness height dependence needs further investigation.

Bubble-Ring Cavitation Scaling

In another recent development,[9] a theory was formulated for the onset of bubble-ring cavitation. The predictions of the theory show promising agreement with the most comprehensive and consistent body of data now available for desinent cavitation on hemispherical headforms when bubble-ring cavitation is present.[8] The theory, which proceeds from first principles insofar as possible, attempts to account for the influence of the laminar separation bubble and for both vaporous and gaseous microbubble growth in the boundary layer of the body. For hemispherical headforms, the laminar separation bubble is calculated to be present at Reynolds numbers, based on headform diameter, as high as 5×10^6 (Ref. 7).

In the theory, the influence of the laminar bubble is accounted for by its maximum height as measured by Arakeri[10]

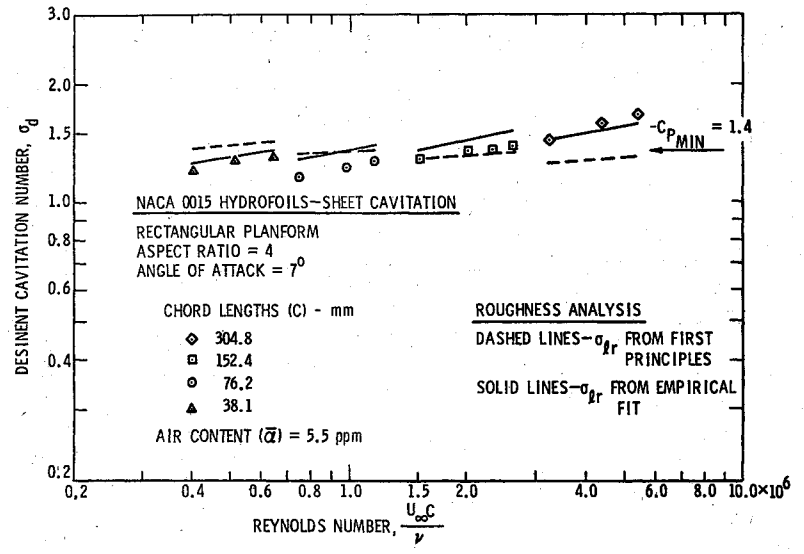

Fig. 1 Analysis of roughness effect on sheet cavitation—NACA 0015 hydrofoils.

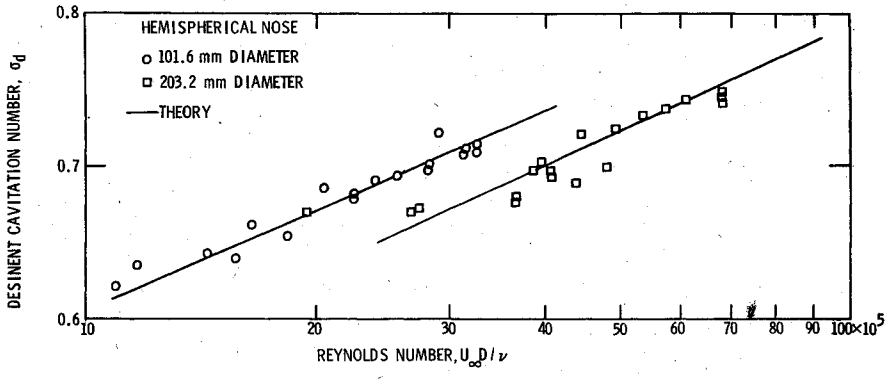

Fig. 2 Analysis of roughness effect on attached-spot cavitation—hemispherical noses.

and Van der Meulen.[11] An analytical approximation for the observed trends, which sets the maximum height of the laminar bubble equal to the maximum diameter of a vaporous cavitation bubble, enables us to write

$$r_m = 55.5(D/R_0)/Re^{0.79} \tag{13}$$

where r_m is the *maximum dimensionless radius* of a vaporous cavitation bubble, $r_m = R_m/R_0$, D is the headform diameter, R_0 is the radius of a "typical" cavitation nucleus, and Re is the Reynolds number based on headform diameter. On the other hand, the postulates of the theory lead to an approximate relationship for the onset cavitation number (σ) and the dimensionless radius (r_m) which is

$$\sigma + C_{p_s} = -4S/(R_0 \rho U_\infty^2 r_m) \tag{14}$$

where C_{p_s} is the pressure coefficient at the laminar separation point, S is the surface tension, ρ the water density, and U_∞ the freestream velocity. We can eliminate r_m from Eqs. (13) and (14) and write

$$\sigma + C_{p_s} = -0.0721 Re^{0.79}/We^2 \tag{15}$$

where We is the Weber number based on headform diameter

$$We = U_\infty/\sqrt{S/\rho D} \tag{16}$$

An extensive body of data on the onset of cavitation on hemispherical headforms has been available for many years[3]; however, these data are not accompanied by information regarding the value of C_{p_s}. The fact that the laminar bubble can persist to such high Reynolds numbers as 5×10^6 was unknown when these measurements were made. Therefore, one cannot compare these data which were obtained for several headform diameters, several water temperatures, and a range of freestream velocities, directly with Eq. (15) for σ. However, one can investigate the usefulness of the ratio $Re^{0.79}/We^2$ as a possible scaling parameter for these data. In order to do this, the following can be written:

$$\sigma = A - BRe^{0.79}/We^2 \tag{17}$$

Then, if the use of the ratio $Re^{0.79}/We^2$ collapses the data, and if the coefficients A and B can be determined empirically, a useful cavitation scaling rule can be found for these headforms.

The value of C_{p_s}, noted above, is not the only aspect of the test results which is subject to question. At the time of these experiments the various forms of cavitation were not always distinguished on hemispherical noses as nicely as they are today. That is not to say that bubble-ring cavitation was not observed when in fact it was. However, there is some confusion between bubble-ring cavitation and other forms such as band cavitation or patch cavitation, particularly on models of larger diameter. Examples of bubble-ring, band, and patch cavitation on hemispherical noses are shown in Fig. 3. Moreover, for some of the smaller headforms at the lower test speeds, some of the cavitation may have been predominantly gaseous. As a result, the data tend to show considerable scatter and one cannot say at this time which of them are definitely associated with bubble-ring cavitation. However, the observations were restricted to cavitation forms which occurred in the boundary layer on the body. The occurrence of larger traveling bubbles was purposely excluded from all data reported although traveling-bubble cavitation was seen in some tests.

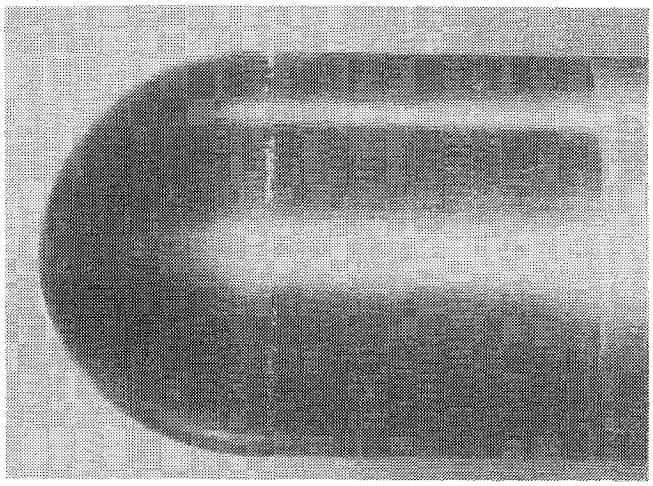

Fig. 3a Bubble-ring cavitation on a hemispherical nose, $D = 50.8$ mm, $U_\infty = 18.2$ m/s, $\sigma = 0.626$.

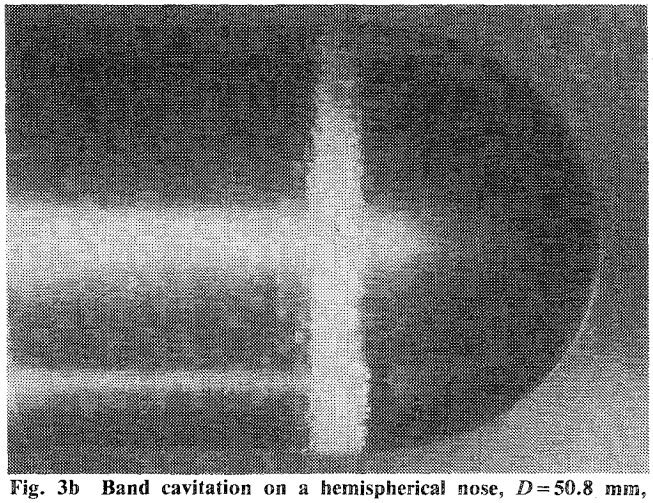

Fig. 3b Band cavitation on a hemispherical nose, $D = 50.8$ mm, $U_\infty = 18.2$ m/s, $\sigma = 0.610$.

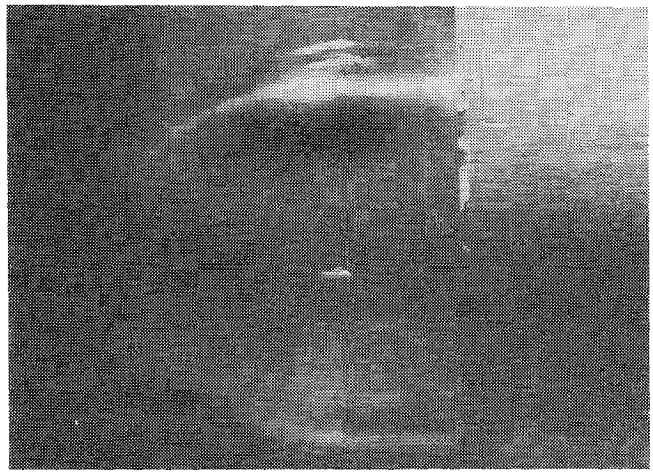

Fig. 3c Patch cavitation on a hemispherical nose, $D = 203.2$ mm, $U_\infty = 21.3$ m/s, $\sigma = 0.772$.

As a result of these deficiencies in the earlier tests, the data show some trends with velocity and body size that are not typical of our present understanding of how bubble-ring cavitation scales. For example, Holl and Carroll[8] report a lower speed limit for bubble-ring cavitation. The existence of this phenomenon of "cavitation cutoff" has been confirmed by independent experiments on bubble-ring cavitation reported by Kodoma[12] which were carried out at about the same time as the work of Holl and Carroll. The older data[3] exhibit no particular cutoff conditions.

By way of contrast, the theory of Ref. 9 predicts the existence of cavitation cutoff. It also shows a limiting higher Reynolds number for bubble-ring cavitation. Thus, a given headform can show bubble-ring cavitation for only a definite range of freestream velocities. Moreover, Eqs. (14) and (15) show that the cavitation number at the onset of bubble-ring cavitation is less than the magnitude of the pressure coefficient at laminar separation and that bubble-ring cavitation is not dependent on air content when this cavitation form is present. Experimental observations, such as those reported by Holl and Carroll,[8] agree with these theoretical findings. However, because of certain approximations contained in Eq. (14), the theory also suggests that experiments carried out on very small headforms in fairly high-speed flows may show somewhat different scaling trends. Therefore, one would not expect Eq. (17) to provide a good guide for cavitation scaling in this case, although just what the limits are in this respect are not presently known.

With the above factors in mind, one can now turn to a consideration of these earlier data in order to test the efficacy of the parameter $Re^{0.79}/We^2$ for cavitation scaling. The data tabulated by Parkin and Holl[3] for hemispherical headforms which range from 28.6 to 101.6 mm diam are shown in Fig. 4 where the desinent cavitation number is plotted against the parameter $Re^{0.79}/We^2$. This figure shows data taken at CIT and ORL. The CIT data were obtained by Kermeen.[13] Evidently the scaling parameter seems to work fairly well for all data taken at a given laboratory. Although the CIT and ORL data seem to show rather close agreement, the CIT data appear to lie slightly above the ORL data. Figure 5 compares the CIT and ORL data for the 12.7 mm diam headform. Again, the CIT data appear to lie consistently above the ORL data, especially at the higher values of $Re^{0.79}/We^2$ (lower freestream velocities) where the effects of gaseous cavitation may have been more pronounced. Also, the scaling parameter seems to work fairly well. The data for the 12.7 mm hemisphere definitely seem to lie below the trends for the larger headforms of Fig. 4, indicating that the scaling parameter fails to bring the data for the smallest headform into alignment with the scaling trends for the larger headforms.

The preceding data were taken under conditions in which water temperature variations were not very large. For this reason, Holl conducted some additional scaling experiments other than those reported in Ref. 3 using colder water. These data, obtained in 1956, are named "ORL Cold Test" and have not been published to date. The temperature range for these data was 13-16.7°C. Figure 6 is a plot of cold test data and the ORL data tabulated in Parkin and Holl.[3] Wherever possible, the data plotted here are averages of the several ordinates when the measured points have a common abscissa. This figure shows that the cold test data definitely lie below the previous ORL data. Therefore, the scaling parameter does not work too well for cases in which the temperature changes significantly. Moreover, the models ranged in size from 12.7 to 203.2 mm diam. This lack of correlation of these data may be partly attributable to headform size as well as changes of water temperature. The separate trends from these averaged data are shown in Fig. 7, which has a magnified vertical scale in order to permit easy comparisons of the effects of size and temperature. The scaling parameter certainly does not collapse the data to a single trend. We must conclude, therefore, that the parameter $Re^{0.79}/We^2$ is not particularly useful as a scaling parameter for cavitation onset on hemispherical headforms, at least insofar as these early data are concerned, and the caveats noted at the start of this section must be taken seriously. Certainly, the fact that there is a sensitivity to temperature variations strengthens this finding.

On the other hand, Parkin and Holl[3] observed that the Weber number itself seemed to be a rather good scaling parameter for the ORL data. A plot showing both cold test

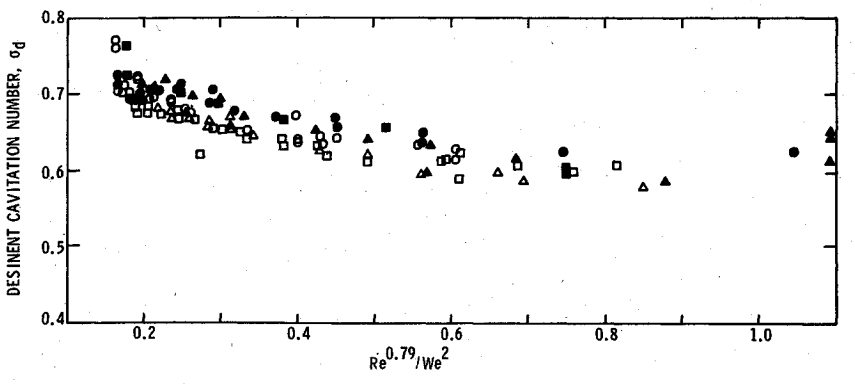

Fig. 4 Analysis of laminar separation effects on hemispherical noses.[3]

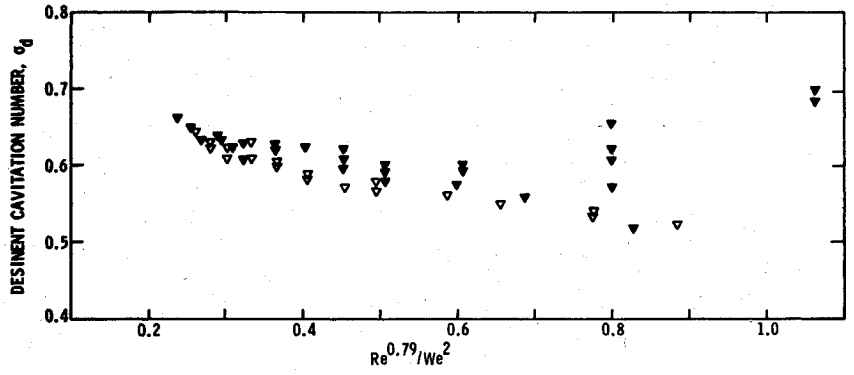

Fig. 5 Analysis of laminar separation effects on 12.7-mm-diam hemispherical nose.

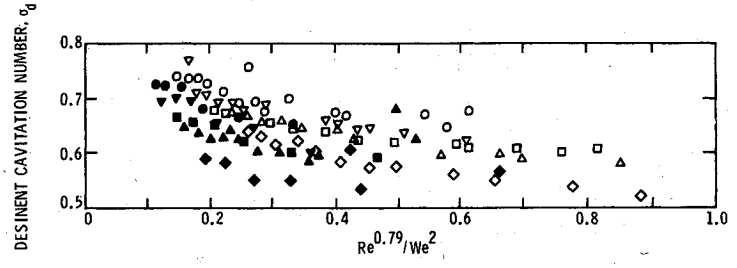

Fig. 6 Analysis of laminar separation effects on both ORL and ORL cold test data on hemispherical noses, Pt. 1.

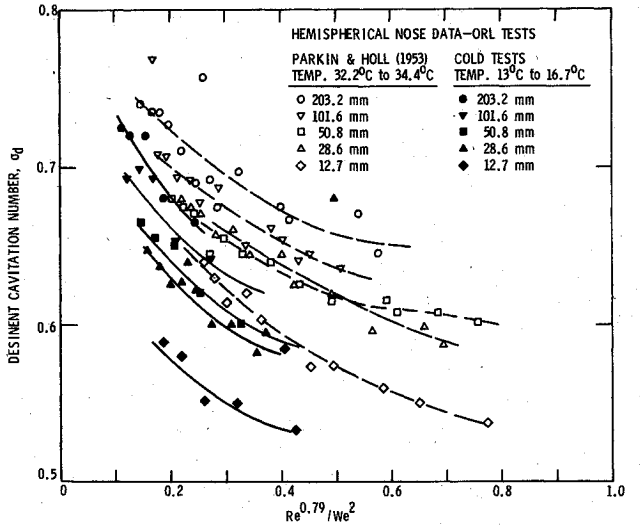

Fig. 7 Analysis of laminar separation effects for both ORL and ORL cold test data on hemispherical noses, Pt. 2.

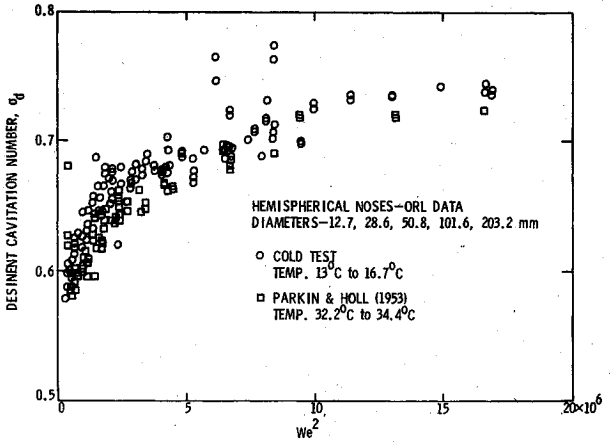

Fig. 8 Correlation of data on hemispherical noses with Weber number.

data and the previous ORL data with no averaging is given in Fig. 8. This graph of σ vs We^2 shows that the ORL data tend to lie slightly below the cold test data, although this slight difference is somewhat overemphasized by the highly magnified vertical scale used in the illustration. In conclusion, this correlation is about as good as found thus far and it is certainly superior to that suggested by Eq. (17). However, since the recent work of Holl and Carroll[8] shows that $C_{p_s} \approx -0.63$ for hemispherical headforms, it seems likely that these early data are not due to a predominance of bubble-ring cavitation. All graphs show many points for which $\sigma > -C_{p_s}$ so that the use of $Re^{0.79}/We^2$ is simply not appropriate for these data. However, the parameter We^2 works quite well, as noted by Parkin and Holl[3] many years ago.

Summary and Conclusions

Possible scaling relationships are presented for two specific types of cavitation—attached-spot and bubble-ring. The analysis of roughness scale effects does appear to correlate the limited amount of data available. With respect to the earlier data on hemispherical headforms, the results of the bubble-ring scaling relationship are not fully understood due to a lack of documentation on the type of cavitation that occurred. This emphasizes the importance of clearly documenting the observed physical characteristics of the cavitation.

The following conclusions can be made about the two proposed cavitation scaling relationships:

1) The roughness formulation given by Eq. (9), which contains Reynolds number (Re) and relative roughness height (h/L) as scaling parameters, predicts the same general characteristics as that shown by several sets of experimental data.

2) Equations (11) and (12) correlate the experimental data for attached-spot cavitation observed on NACA 0015 hydrofoils and hemispherical noses, respectively.

3) The scaling formulation proposed by Eq. (17) introduces the ratio $Re^{0.79}/We^2$ for correlating bubble-ring-type cavitation.

4) When this ratio is applied to previous data for desinent cavitation on hemispherical headforms, it is found that these data do not correlate as well as when the single parameter We^2 is employed. Causes for this state of affairs are presently unknown. The asymptotic theory, which underlies the ratio $Re^{0.79}/We^2$, applies strictly to bubble-ring cavitation, and then only to those flows for which the time spent by a nucleus in the region favorable to vaporous growth is much greater than the characteristic time for microbubble response to an external disturbance. This rules out those flows at high speeds around very small models. This could be one factor contributing to certain deficiencies noted in the correlations attempted in this paper. Another could be that these early data contain other forms of surface cavitation besides bubble-ring cavitation, in which case one cannot expect the ratio to apply. Since many of these data appear to show desinent cavitation numbers that exceed the magnitude of the pressure coefficient at the laminar separation point C_{p_s}, then either the theory is incorrect for bubble-ring cavitation or, as indicated previously, other forms of cavitation may have been observed in the earlier tests. However, the theory is in good agreement with the most completely documented set of data on bubble-ring cavitation.[8]

Acknowledgments

The research was sponsored by the Naval Sea Systems Command, Codes NSEA 63R-31 and NSEA-05H.

References

[1] Holl, J. W., "The Inception of Cavitation on Isolated Surface Irregularities," *Journal of Basic Engineering, Transactions of ASME,* Vol. 82, 1960, pp. 169-183.

[2] Arndt, R. E. A., Holl, J. W., Bohn, J. C., and Bechtel, W. T., "The Influence of Surface Irregularities on Cavitation Performance," *SNAME, Journal of Ship Research,* Vol. 23, No. 3, Sept. 1979, pp. 157-170.

[3] Parkin, B. R. and Holl, J. W., "Incipient-Cavitation Scaling Experiments for Hemispherical and 1.5 Caliber Ogive-Nosed Bodies," Report NOrd 7958-264, Ordnance Research Laboratory, The Pennsylvania State University, May 1953. (The Ordnance Research Laboratory [ORL] is now known as the Applied Research Laboratory [ARL])

[4] Holl, J. W. and Wislicenus, G. F., "Scale Effects on Cavitation," *Journal of Basic Engineering, Transactions of ASME,* Series D, Vol. 83, Sept. 1961, pp. 385-398.

[5] Parkin, B. R., "Scale Effects in Cavitating Flow," Ph.D. Dissertation, California Institute of Technology, 1952.

[6] Billet, M. L. and Holl, J. W., "Scale Effects on Various Types of Limited Cavitation," *Proceedings of the International Symposium on Cavitation Inception,* ASME, New York, N. Y., Dec. 1979, pp. 11-24.

[7] Arakeri, V. H. and Acosta, A. J., "Viscous Effects in the Inception of Cavitation on Axisymmetric Bodies," *Journal of Fluids Engineering, Transactions of ASME,* Vol. 95, Series 1, No. 4, Dec. 1973, pp. 519-528.

[8] Holl, J. W. and Carroll, J. A., "Observations of the Various Types of Limited Cavitation on Axisymmetric Bodies," *Proceedings of the International Symposium on Cavitation Inception,* ASME, New York, N. Y., Dec. 1979, pp. 87-100.

[9] Parkin, B. R., "A Theory for Cavitation Inception in a Flow Having Laminar Separation," ARL Tech. Memo. No. 79-198, Nov. 1979.

[10] Arakeri, V. H., "Viscous Effects in Inception and Development of Cavitation on Axisymmetric Bodies," Ph.D. Thesis, California Institute of Technology, 1973; also released as Report No. 3183.1, Division of Engineering and Applied Science, California Institute of Technology, 1973.

[11] Van der Meulen, J. H. J., "A Holographic Study of Cavitation on Axisymmetric Bodies and the Influence of Polymer Additives," Netherlands Ship Model Basin, Wageningen, The Netherlands, Publ. No. 509, 1976.

[12] Kodoma, Y., private communication from Japan Ship Research Institute, Dec. 1979.

[13] Kermeen, R. W., "Some Observations of Cavitation on Hemispherical-Head Models," Hydrodynamics Laboratory, California Institute of Technology, Rept. E-35.1, June 1952.